0013-7227/02/$15.00/0
Printed in U.S.A.

Endocrinology 143(7):2599–2609

Thrittene, Homologous with Somatostatin-28$_{(1–13)}$, Is a Novel Peptide in Mammalian Gut and Circulation

JOHN W. ENSINCK, DENIS G. BASKIN, TORSTEN P. VAHL, ROBIN E. VOGEL, ELLEN C. LASCHANSKY, BRUCE H. FRANCIS*, ROSS C. HOFFMAN†, JONATHAN D. KRAKOVER‡, MICHAEL R. STAMM, MALCOLM J. LOW, MARCELO RUBINSTEIN§, VERONICA OTERO-CORCHON, AND DAVID A. D'ALESSIO

Division of Metabolism, Endocrinology, and Nutrition, Department of Medicine (J.W.E., D.G.B., R.E.V., E.C.L., B.H.F.) and Department of Biological Structure (D.G.B.), University of Washington, Seattle, Washington 98195; Department of Veterans Affairs Puget Sound Health Care System (D.G.B.), Seattle, Washington 98108; ZymoGenetics (R.C.H., J.D.K., M.R.S.), Seattle, Washington 98102; Vollum Institute (M.J.L., M.R., V.O.-C.), Oregon Health Sciences University, Portland Oregon 97201-3098; and Division of Endocrinology (T.P.V., D.A.D.), University of Cincinnati, Ohio 45267-0547

Preprosomatostatin is a gene expressed ubiquitously among vertebrates, and at least two duplications of this gene have occurred during evolution. Somatostatin-28 (S-28) and somatostatin-14 (S-14), C-terminal products of prosomatostatin (ProS), are differentially expressed in mammalian neurons, D cells, and enterocytes. One pathway for the generation of S-14 entails the excision of Arg^{13}-Lys^{14} in S-28, leading to equivalent amounts of S-28$_{(1–12)}$. Using an antiserum (F-4), directed to the N-terminal region of S-28 that does not react with S-28$_{(1–12)}$, we detected a peptide, in addition to S-28 and ProS, that was present in human plasma and in the intestinal tract of rats and monkeys. This F-4 reacting peptide was purified from monkey ileum; and its amino acid sequence, molecular mass, and chromatographic characteristics conformed to those of S-28$_{(1–13)}$, a peptide not described heretofore. When extracts of the small intestine were measured by RIA, there was a discordance in the ratio of peptides reacting with F-4 and those containing the C terminus of ProS, suggesting sites of synthesis for S-28$_{(1–13)}$ distinct from those for S-14 and S-28. This was supported by immunocytochemistry, wherein F-4 reactivity was localized in gastrointestinal (GI) endocrine cells and a widespread plexus of neurons within the wall of the distal gut while immunoreactivity to C-terminal domains of S-14 and S-28 in these neurons was absent. Further, F-4 immunoreactivity persisted in similar GI endocrine cells and myenteric neurons in mice with a targeted deletion of the preprosomatostatin gene. We believe that these data suggest a novel peptide produced in the mammalian gut, homologous with the 13 residues of the proximal region of S-28 but not derived from the ProS gene. Pending characterization of the gene from which this peptide is derived, its distribution, and function, we have designated this peptide as thrittene. Its localization in both GI endocrine cells and gut neurons suggests that thrittene may function as both a hormone and neurotransmitter. (*Endocrinology* 143: 2599–2609, 2002)

PREPROSOMATOSTATIN (PreproS) is a gene that is widely expressed in vertebrates, including mammals, birds, reptiles, amphibians, and fish. Elements of the PreproS sequence are among the most highly conserved in vertebrate evolution, suggesting important regulatory roles for its peptide products (1). In addition, there seems to have been at least two duplications of PreproS over the course of evolution (1, 2). Teleost fish and amphibians express two PreproS genes, and the recently discovered preprocortistatin is a novel mammalian gene that is thought to be a member of the somatostatin peptide family (3, 4). In mammals, PreproS is translated into the 92 residue prohormone, prosomatostatin (ProS), which includes two bioactive peptides at its C terminus: somatostatin-14 (S-14) and somatostatin-28 (S-28). These peptides are uniquely processed and differentially secreted from cells in the brain, pancreatic islets, and gastrointestinal (GI) tract, where they act through specific membrane receptors to inhibit the release of neurotransmitters and hormones within the central nervous system (CNS) and gastroenteropancreatic (G-E-P) system (5, 6).

The intracellular generation of S-28 and/or S-14 is dependent on specific endoproteases that cleave ProS at designated sites (7). The processing of ProS is differentially regulated in the cells that produce it. In intestinal endocrine cells, S-28 along with equimolar amounts of ProS$_{(1–64)}$ are generated (8). By contrast, S-14 is formed in gastric and islet D cells and a subset of enteric neurons. Both S-28 and S-14 are found in specific populations of neurons in the CNS. Processing of ProS to S-14 can occur directly with the coformation of equimolar amounts of ProS$_{(1–76)}$ or indirectly from cleavage of S-28. In the latter case, S-28$_{(1–12)}$ is also produced (9–16). Thus, the intracellular cleavages of ProS are complex, with potential for differential regulation among ProS-containing cells, leading to different products. In this setting, we have produced an antiserum (F-4) with a high avidity for S-28, but little for S-28$_{(1–12)}$, and none for S-14 (S-28$_{(15–28)}$), thereby allowing the development of a sensitive RIA for the former peptide (17). Using this assay, we have found a peptide distinct from S-28 in plasma and intestinal tissues. This peptide has been purified from extracts of monkey ileum, where

Abbreviations: CH_3CN, Acetonitrile; CNS, central nervous system; G-E-P, gastroenteropancreatic; GI, gastrointestinal; HAc, acetic acid; MALDI-TOF, matrix-assisted laser desorption ionization-time of flight; PreproS, preprosomatostatin; ProS, prosomatostatin; PSD, postsource decay; rp, reverse-phase; S-14, somatostatin-14; S-28, somatostatin-28; TFA, trifluoroacetic acid.

it occurred in highest concentration. Its immunological and physical properties are compatible with the structure of S-28$_{(1–13)}$, which has not been previously described as a distinct entity. Furthermore, we have obtained evidence that S-28$_{(1–13)}$ is present in the tissues of PreproS knockout mice, indicating that this peptide is not a product of ProS. Because we have been unable to find evidence, in available data banks, for genes other than PreproS that have homology with the nucleic acid sequence corresponding to S-28$_{(1–13)}$, we propose that this peptide, which we have tentatively named thrittene, is a novel product derived from a hitherto unrecognized gene.

Materials and Methods

Peptides and antisera

S-28, S-28$_{(1–12)}$, Tyr^{14}-S-28$_{(1–14)}$, and Tyr^{1}-S-28$_{(1–14)}$, were purchased from Peninsula Laboratories, Inc. (Belmont, CA). S-28$_{(1–13)}$ was custom synthesized at ZymoGenetics (Seattle, WA). ProS, partially purified from rat brain, was a gift from Dr. Robert Benoit, the Montreal General Hospital Research Institute. The tyrosinated peptides (1–5 μg) were coupled with Na^{125}I (Amersham Pharmacia Biotech, Arlington Heights, IL) and purified as previously described (17). Tyr^{14}-S-28$_{(1–14)}$ was linked to Tyr residues in bovine thyroglobulin by diazotization. Approximately 30 μg peptide were emulsified in incomplete Freund's adjuvant and injected intradermally, at 10–20 sites, into each of 10 young female New Zealand white rabbits. The animals received repeat injections at 3-month intervals, after approval of the University of Washington Animal Research Committee. The antiserum, given the trivial designation of F-4, was tested for titer, specificity, and avidity by comparing the binding by RIA of several synthetic peptides with sequential amino acid deletions from the N and C terminus of S-28 and S-28$_{(1–14)}$, respectively (17). F-4 interacts predominately with the Asn^{5}-Pro^{6} sequence of S-28. In addition, 2 polyclonal antisera (designated AS-10 and AS-77) and a monoclonal Ig termed MS-12 were generated, with S-14 as the antigen, under conditions previously reported (17, 18). AS-10 and MS-12 interact with the Phe^{7}-Trp^{8}-Lys^{9} region of S-14, whereas AS-77 binds to the Ala^{1}-Ser^{2} residues of the peptide. Antiserum Kiisha, generated against a synthetic peptide containing the 14 N-terminal amino acids of ProS, was a gift from Dr. Bernard Roos, University of Miami (19). Antiserum CTP was created in rabbits using a synthetic peptide corresponding to ProS$_{(33–45)}$ (17). Antiserum S-320, which reacts with S28$_{(1–12)}$ (20), was kindly donated by Dr. Robert Benoit. The epitopes along ProS where these antisera interact are schematized in Fig. 1.

RIA

The optimal conditions for equilibration binding of the radioligands with their respective antisera have been previously published (17). The F-4 RIA was carried out in 50 mM barbital buffer, pH 8.0, containing 0.25% BSA and thiomerosal (1:10,000 final concentration). Buffer (0.9 ml) was mixed with 0.05 ml antiserum (1:8,000 final concentration); and variable volumes of solution containing either reference standards or unknown samples were added. Inhibitors of proteolytic enzymes were not routinely included because degradation of peptides was not found in plasma or tissue extracts. After incubation for 24 h at 4 C, 0.05 ml I^{125}Tyr^{1}S-28$_{(1–14)}$, purified by gel filtration, was added and the reaction carried out for an additional 48 h. Bound tracer was precipitated with 1 ml 30% polyethylene glycol (Carbowax 8000; Great Western Chemical, Seattle, WA) after addition of 1 mg purified γ-globulin (fraction 2; Sigma, St. Louis, MO).

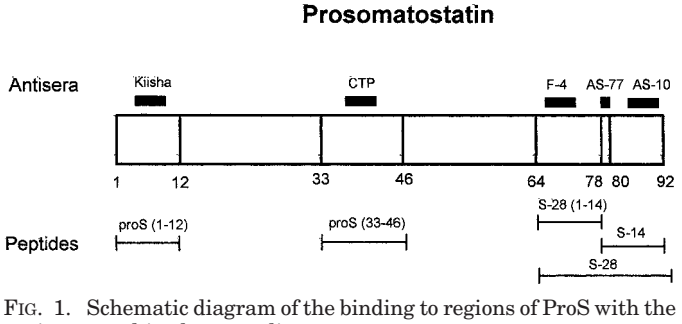

FIG. 1. Schematic diagram of the binding to regions of ProS with the antisera used in these studies.

Human subjects

Forty lean, healthy men (age range, 22–50 yr), not taking medication, gave informed consent and signed forms approved by the University of Washington Institutional Review Board. Thirty subjects had a single 10-ml sample of blood withdrawn after an overnight fast. To prevent degradation of peptides by endo- and exopeptidases, blood was collected on ice, the plasma separated, the pH adjusted to 3, with 1 N HCl (17), and it was stored at −80 C. For routine analyses, 5-ml aliquots of acidified plasma were filtered through cartridges containing octadecylsilyl silica (Sep-Pak; Waters Corp., Milford, MA) and were washed sequentially with 5 ml H_2O and 5 ml 0.1% trifluoroacetic acid (TFA) in H_2O, and the retained peptides were eluted with 5 ml of a solution of 80% methanol and 1% TFA. The eluates were air-dried and dissolved in 2 ml assay buffer. Recoveries of S-28 and S-28$_{(1–13)}$ (50–100 pg), added to 5 ml of acidified plasma, were 78 ± 2% (n = 15) and did not vary significantly from each other. Twenty milliliters of acidified plasma from six fasting volunteers were processed through Sep-Pak and underwent gel filtration chromatography (see below). Ten fasting subjects had 250 ml blood taken. The acidified plasma was pooled and then processed sequentially through Sep-Pak, an F-4 immunoadsorbent, and gel filtration chromatography, and the eluates were submitted to HPLC (see below).

Animal tissue extraction

G-E-P organs were obtained from anesthetized young monkeys (*Macaca nemestrina*), mature Wistar rats, and C57BL/6J wild-type (*Smst* +/+) and ProS knockout mice (*Smst* −/−) (21), following procedures approved by the University of Washington Animal Research Committees. For extraction of peptides, monkey tissue was dissected and placed on ice. The intestine was arbitrarily transected into segments corresponding to the duodenum, jejunum, ileum, and colon. The lumens of the organs were quickly washed with cold 0.15 M NaCl, and all tissues were snap-frozen in liquid nitrogen and stored at −80 C. In larger scale extraction, ileum from eight juvenile monkeys was processed as above. The frozen tissue was pulverized in a steel cylinder in liquid nitrogen and dropped into boiling 2 N acetic acid (HAc) for 5 min. After cooling and homogenization with a glass rod, the solution was centrifuged at 30,000 × *g* and the supernatant decanted and lyophilized. The residue was weighed, and a small portion was dissolved in water for protein determination by the Folin method or using the bicinchohonic kit technique (Pierce Chemical Co., Rockford, IL). Overnight fasted, male Wistar rats (250–300 g) were killed with ip nembutal; and tissue segments corresponding to stomach, duodenum, jejunum, and ileum were rapidly removed and the mucosal surfaces separated from the adjacent submucosa and muscularis layers by stripping with a microscopic slide. The separate layers were then immersed in boiling 2 N HAc and processed as outlined above. *Smst* +/+ and *Smst* −/− mice were killed; and pancreas, stomach, and segments of the upper and lower intestine were removed to liquid nitrogen before storage at −80 C. These tissues were also extracted in 2 N HAc and processed through Sepak cartridges, and the reconstituted eluates were passed through a 45-μm filter before HPLC.

Affinity chromatography

The F-4 antiserum was coupled to cyanogen bromide-activated Sepharose 4B as detailed elsewhere (17). For immunoadsorption of peptides from plasma or tissue extracts, reference peptides, or unknown samples, diluted in 2 ml 130-mM phosphate buffer, pH 8.5, were introduced into 5 × 1-cm syringes containing the gel in buffer, washed with borate, and the F-4 reacting peptides were eluted with 0.2 N HAc, pH 3.5, containing BSA and lyophilized.

Gel permeation chromatography

Chromatography was carried out in columns (1.5 × 90 cm) containing Bio-Gel P-10 (200–400 mesh) (Bio-Rad Laboratories, Inc., Chemical Division, Richmond, CA) equilibrated in 50 mM borate buffer, pH 8.5, containing 0.25% BSA. The columns were calibrated with blue dextran with molecular mass exceeding 1000 kDa; cytochrome c (Sigma) with molecular mass of 13 kDa; S-28 with molecular mass of 3.1 kDa; S-14 with molecular mass of 1.6 kDa; S-$28_{(1–13)}$ with molecular mass of 1.4 kDa; and ^3H_2O. Filtration occurred under gravity, at room temperature, at 10 ml/h; and 1-ml fractions were automatically collected.

HPLC

Chromatography of plasma, after immunoadsorption, was performed in a modular HPLC system (Spectra-Physics, San Jose, CA). Samples (0.15–1.0 ml) were injected onto a micron analytical column (Vydac C-18 5; The Separations Group, Hesperia, CA) and eluted with sequential gradients consisting of acetonitrile (CH_3CN)/0.1% TFA: first, a 0–20% solution, stepped over 10 min; followed by a 20–30% step over 10 min; then a 30–40% linear gradient for 70 min; and, lastly, a 40–90% linear gradient for 30 min. The flow rate was 0.5 ml/min. Separation of mouse tissue extracts used a similar buffer/solvent combination, with a gradient of: 5–20% over 20 min, 20–37% over 70 min, and 37–90% over 20 min.

Preparative reverse-phase (rp) HPLC of tissue extracts was performed on a 4.6 × 150-mm, PLRP-S 100 A, 5-μm column (Polymer Laboratories Inc., Amherst, MA) using an integrated HPLC system (Perspective BioSystems, Framingham, MA). A flow rate of 1 ml/min was used, and an isocratic of 1% B for 10 min, followed by a 1–41% gradient over 80 min, was initiated upon injection, where A is 2% CH_3CN + 4 mM NH_4Ac, pH 10, and B is 90% CH_3CN + 4 mM NH_4Ac, pH 10. Microbore rp HPLC was carried out on an Ultrafast Microprotein Analyzer (Michrom BioResources Inc., Auburn, CA). A 1 × 150-mm C_{18} 300 A, 5-μm column (Vydac, Hesperia, CA) was used at a flow rate of 50 μl/min at 30 C. A gradient of 1–41% over 80 min was begun on injection, where A is 2% CH_3CN + 0.1% TFA and B is CH_3CN + 0.095% TFA.

N-terminal sequence analysis

N-terminal sequence analysis was performed on a protein sequencer (Model 476A; PE Applied Biosystems, Foster City, CA); and data analyses on a Model 610A Data Analyses System (also PE Applied Biosystems). Thirty and 50 μl of the respective microbore fractions were analyzed.

Matrix-assisted laser desorption ionization-time of flight (MALDI-TOF) mass spectrometry

MALDI-TOF mass spectra of peptides were obtained with a TofSpec SE mass spectrometer (MicroMass, Beverly, MA) equipped with a 337-nm laser. Linear positive-ion experiments were performed with the suppression mass at 400 Da and the following voltages: source, 25,000 V; extraction, 8,333 V; focus, 23,000 V; and linear detector, 3,800 V. Postsource decay (PSD) positive-ion experiments were performed with the suppression mass at 500 Da, the BN gate set to the ion of interest, and the following voltages: source, 25,000 V; extraction, 8,333 V; focus, 23,000V; reflectron voltage at 28,575 V; and reflectron detector at 1,800 V. The instrument had a 0.5% accuracy (±7 Da) for an externally calibrated sample and approximately 0.1% accuracy (±1.5 Da) for internally calibrated samples.

Immunocytochemistry

Rats and mice were anesthetized and perfused with 4% paraformaldehyde in 100 mM phosphate buffer, pH 7.4. Fresh tissue samples from rodents and monkeys were immersed in fresh fixative overnight, at 6 C, and then placed in 50 mM cold phosphate buffer containing 25% sucrose, for 24 h. Some of the tissue samples were frozen and cut, by cryostat, into 7-μm sections; others were immersed sequentially through ethanol and toluene, embedded in paraffin, and cut into 5-μm sections. Immunostaining of cryostat and paraffin sections was performed by the same procedure, except that the paraffin was removed with xylene and ethanol beforehand. For fluorescence immunostaining (22, 23), sections were placed in 10 mM phosphate buffer, pH 7.4, containing 5% normal goat serum, followed by immersion in primary antiserum, overnight, at 6 C. Primary antisera were diluted in 10 mM phosphate buffer, pH 7.4, according to the following: F-4, 1:2000; AS-10, 1:1000; MS-12, 1:1000; AS-77, 1:1000, CTP, 1:2000; and Kiisha (N-terminal ProS antiserum), 1:1000. After a rinse in cold buffer, sections were immersed for 1 h in goat antirabbit IgG (for MS-12) conjugated to Cy3 (for polyclonal antisera) or goat antimouse IgG conjugated to Cy3 (Jackson ImmunoResearch Laboratories, Inc., West Grove, PA) diluted to 1:200 in phosphate buffer. For bright-field immunostaining, sections were treated with the antisera and then processed with the Vectastain Elite ABC kit (Vector Laboratories, Inc., Burlingame, CA), using IgG-biotin-streptavidin reagents for diaminobenzidine staining. Controls for immunocytochemistry included: 1) omission of all primary and secondary antibodies; 2) omission of primary antibodies only, with substitution of normal rabbit (or mouse) serum; 3) staining of pancreatic D cells (known to express ProS); and 4) examination with fluorescence excitation and emission filters that do not excite and transmit Cy3 fluorescence. Because all of these primary antisera have been extensively characterized for specificity by RIA analyses (17), and absorption controls for AS-10 and F-4 have been previously reported (22, 23), they were not repeated in this study.

Results

Characterization of F-4 antiserum interacting with ProS and its C-terminal sequences

The binding characteristics of F-4 with ProS, S-28, S-$28_{(1–14)}$, S-$28_{(1–13)}$, S-$28_{(1–12)}$, and S-14 are shown in Fig. 2. F-4 interacted with ProS, S-28, and S-$28_{(1–14)}$ with similar avidity, permitting their detection in the femtomolar range. Noteworthy, the cross-reactivity of this antiserum with S-$28_{(1–12)}$ was extremely poor, whereas S-$28_{(1–13)}$ had the highest affinity of all peptides tested. S-$28_{(1–13)}$ was bound to F-4 50- to 100-fold more avidly than S-28 throughout the range of concentrations tested. This implies that modifications of the C-terminal structure of the antigen, S-$28_{(1–14)}$, markedly affect the binding to F-4. From previous studies using synthetic peptides with sequential amino acid deletions from the N terminus of S-28, we infer

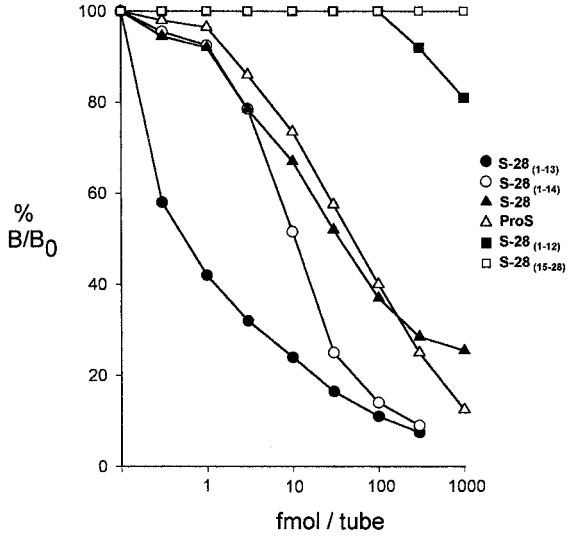

FIG. 2. Immunologic interactions of ProS and related peptides with antiserum F-4 using ^{125}I-Tyr-S-$28_{(1–14)}$ as radioligand. Data are presented as % B/B_0, the amount of iodinated tracer bound at each peptide concentration relative to tracer binding without added peptide.

that the Asn^5-Pro^6 sequence is necessary for binding to F-4 (17). The lowest limits of detection of $S\text{-}28_{(1–13)}$ and S-28 in the RIA were 0.2 and 2 fmol per tube, with interassay variances of 15% (n = 10) and intraassay variances of 8% and 5% (n = 10), respectively.

Measurement of peptides reacting with F-4 antiserum in fasting human plasma

As previously reported (17), we quantified S-28 levels in human plasma by passing Sep-Pak eluates through an F-4-agarose immunoadsorbent to adhere the peptide at its Asn^{-5}-Pro^6 epitope and using AS-10 RIA to measure the Phe (21)-Trp (22)-Lys^{23} region of S-28 in the fractions eluted with HAc. We also measured the levels of all F-4 reactive substances in the acid eluates using S-28 as standard. The values for S-28 and the substances registered in the F-4 RIA in fasting plasma samples of 30 healthy subjects are compared in Fig. 3. The levels of S-28 ranged between 5 and 27 pg/ml, with a mean of 14.5 ± 0.9 pg/ml, whereas the values for the substances reacting with F-4 varied from 37–200 pg equivalent amounts of S-28/ml, with a mean of 110 ± 9. This highly significant difference ($P < 0.001$) suggests that F-4 binds to peptides other than S-28 in human plasma.

To determine whether substances measured by F-4 in plasma might be distinguished by molecular size, 70 ml plasma from each of six fasting men were separately passed through Sep-Pak and (after the adhered peptides were eluted with CH_3CN, lyophilized, and solubilized in buffer) passed through the F-4 affinity column. This latter step eliminates S-14, because this peptide is not bound to F-4. The adsorbed peptides were eluted with 2 N HAc, neutralized, and then filtered through BioGel P-10 in 50 mM borate buffer, pH 8.5. The collected fractions were assayed by RIAs using F-4 and AS-10. A profile of one subject, representative of all six men, is depicted in Fig. 4. Two separate peaks detected by F-4 RIA are evident. One corresponds to the elution behavior of cytochrome c (molecular mass, 13 kDa), and a second (more diffuse) area overlaps the behavior of synthetic standards for $S\text{-}28_{(1–13)}$ (molecular mass, 1400 Da) and S-28 (molecular mass, 3149 Da). AS-10 immunoreactivity corresponded with the F-4 immunoreactive peaks at the cytochrome c and S-28 markers, and we infer that these represent ProS and S-28, respectively. The larger F-4 reacting peak that was not detected using the AS-10 coeluted with the $S\text{-}28_{(1–13)}$ standard. The precedence of synthetic $S\text{-}28_{(1–13)}$ over S-28 under these conditions of molecular sieving presumably reflects the elongated molecular conformation, and Stokes' radius of this peptide contrasted with the more helical configuration of S-28 because of the disulfide linkage at residues 17 and 28.

In an attempt to further resolve the properties of the components of this peak, a 1-liter pool of plasma from 10 men was processed through Sep-Pak, F-4 immunoadsorption, and filtration on BioGel. The second peak from BioGel was pooled, concentrated through Sep-Pak, and submitted to HPLC. As shown in Fig. 5, two distinct peaks were identified by F-4 RIA consistent with the elution characteristics of synthetic $S\text{-}28_{(1–13)}$ and S-28, respectively. The first peak was not detected using the AS-10 RIA, indicating an absence of the C-terminal epitope recognized by this antiserum, and consistent with the structure of $S\text{-}28_{(1–13)}$. The material in the second peak was detected in the AS-10 assay, indicating an identity of S-28.

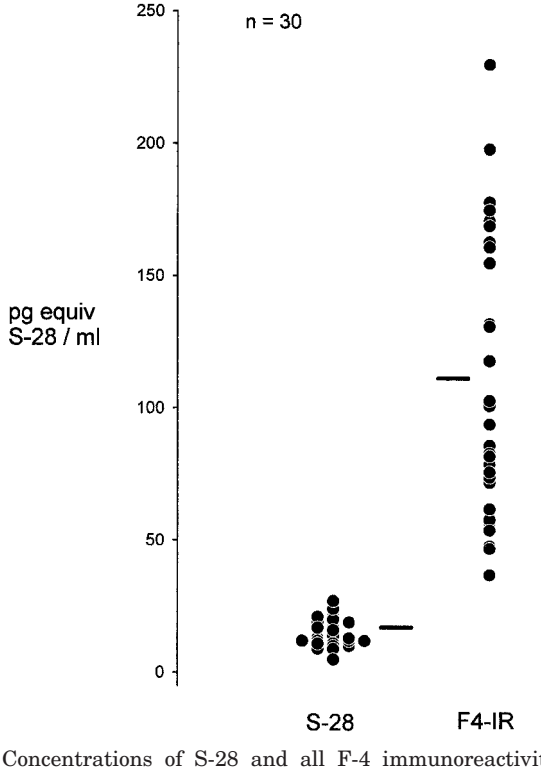

FIG. 3. Concentrations of S-28 and all F-4 immunoreactivity, in healthy men, after an overnight fast. Peptides from plasma (5 ml) were adsorbed and eluted from Sep-Pak. S-28 was quantified by F-4 immunoadsorption and measurement of the C-terminal region by AS-10 antiserum. The F-4 immunoreactive peptides (F-4 IR) were measured directly in the Sep-Pak eluates.

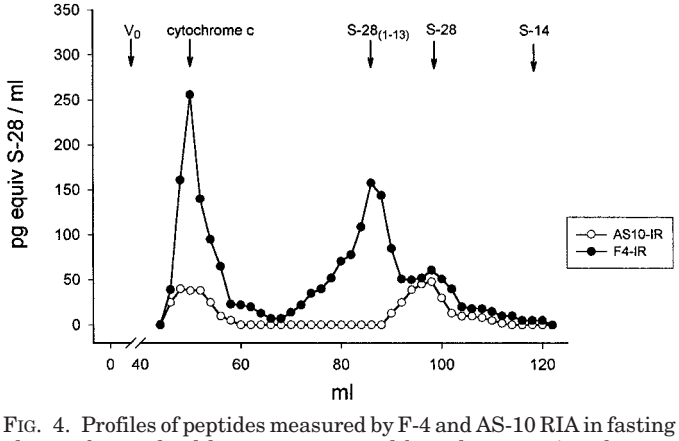

FIG. 4. Profiles of peptides measured by F-4 and AS-10 RIA in fasting plasma from a healthy man, separated by gel permeation chromatography. Plasma (70 ml) was adsorbed to Sep-Pak and eluted, and the eluates dissolved in borate buffer were subjected to immunoadsorption on F-4 agarose. The retained peptides were eluted with 2 N HAc, lyophilized, and reconstituted in 1.0 ml borate buffer for application to the column. Filtration was carried out in a 1.5 × 90-cm column containing BioGel P-10 in 50 mM borate buffer, pH 8.5, containing 0.25% BSA. RIA measurements were performed using S-28 as standard. *Arrows*, Peaks where markers of known composition were eluted; V_0, void volume detected by blue dextran; cytochrome c has a molecular mass of 13 Da.

Distribution of F-4 and AS-10 immunoreactive peptides in G-E-P tissues

Based on the presence of F-4 immunoreactivity in plasma and prompt and sustained responses to nutrient ingestion in humans (Ensinck, J. W., unpublished), we reasoned that the principal source(s) of the F-4 reacting peptides was likely to be in the gastrointestines and/or pancreas. Therefore, we systematically extracted the G-E-P organs of four fasted, anesthetized Macaques into boiling HAc and, after lyophylization and resolubilization, measured the amounts of AS-10 and F-4 immunoreactive species in them. Table 1 shows the comparison of the mean concentrations of the peptides detected by the F-4 and AS-10 RIA, expressed as ng equivalent amounts of S-28/mg protein in pancreas, stomach, and small and large intestines. The concentrations of peptides detected by AS-10 RIA were similar in pancreas, stomach, and small intestine, and declined in the colon. Because AS-10 detects ProS and both S-14 and S-28, these findings do not permit assessment of the relative amounts of these peptides in the G-E-P tissues. However, previous studies have shown that S-14 predominates in the D cell of pancreas and stomach and is located in neurons in the small and large intestines, whereas S-28 is the sole ProS-derived peptide in enterocytes functioning as endocrine cells (22, 23). Interestingly, the levels of substances in the G-E-P tissues reacting in the F-4 RIA showed a different pattern, compared with the peptides detected by AS-10. In pancreatic and gastric tissue, concentrations were similar; however, values increased progressively down the small intestine and, in the jejunum and ileum, were 5- to 10-fold greater than those in pancreas and stomach. Not only were the concentrations of peptides measured with F-4 significantly greater in the mid-and distal small gut segments, but also the ratios of F-4 to AS-10 immunoreactive species were markedly increased. This implies that a peptide(s) other than S-28, which has an F-4:AS-10 ratio of 1, was preferentially distributed in these regions of the intestine.

A similar distribution of F-4/AS-10 immunoreactivity was found in the G-E-P tissues of rats. Measurement of these peptides in HAc extracts corresponding to mucosal and submucosal layers of the stomach and intestines indicated that AS-10 immunoreactive peptides were much greater in the gastric and duodenal mucosa than in that of the distal gut, whereas the levels in the submucosa were similar throughout all the tissues. By contrast, F-4 reactivity was disproportionately increased in the ileal mucosal (but not in submucosal) scrapings. We infer from the marked increase in the ratio of F-4 to AS-10 immunoreactive species in the jejunum and ileum, from both the rat and monkey, that the substance in the circulation that is measured by the F-4, but not AS-10, RIA originates from cells in the distal small intestine.

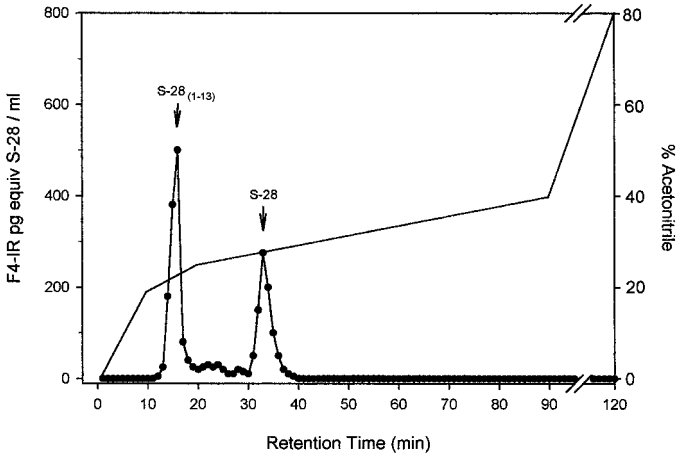

FIG. 5. HPLC profile of F-4 immunoreactive peptides (F-4 IR) from a pool of 1 liter plasma from 10 healthy men after an overnight fast. The plasma was processed as described in Fig. 3. The fractions from tubes 70–110 were pooled, concentrated by Sep-Pak, and lyophilized. The peptides were applied to a C-18 rp column with a variable gradient of CH_3CN in 0.1% TFA. The eluates were analyzed by both F-4 and AS-10 RIA.

Isolation and identification of S-28$_{(1–13)}$ in mammalian gut

To determine the structure of the substance occurring in both plasma and gut that was detected by F-4 RIA but distinct from S-28, monkey ileum was processed as described in *Materials and Methods*. This entailed sequential extraction of freshly obtained gut in boiling HAc, ultracentrifugation to remove sediment, filtration on BioGel P-10, immunoadsorption on F-4 coupled to agarose, preparative rpHPLC at high pH, and microbore rpHPLC at low pH. The F-4 reactive peak from 2 independent runs of the final low-pH rpHPLC step underwent N-terminal sequence analysis and MALDI-TOF mass spectrometry. The sequence derived from the combined analyses revealed 13 residues, with identification of 8 as follows: SXNXNPAMAXXEX. Although 5 of the 13 residues could not be identified, the N-terminal Ser, Asn^3, Asn^5-Pro^6-Ala^7-Met^8-Ala^9, and Glu (12) were arranged in correct sequence for the N-terminal region of S-28. Furthermore, throughout each of the purification steps, the unknown peptide behaved identically to authentic, synthetic S-28$_{(1–13)}$.

The Maldi-TOF MS analysis of the final product of our purification paradigm yielded masses of 1420 Da in 1 preparation and 1419.3 Da in the second. These masses are very similar to the isotopic average mass expected for S28$_{(1–13)}$ with oxidation of the methionine residue at position 8 to methionine sulfoxide-1416.5 Da. A mass error of 0.2% is acceptable for a linear MALDI-TOF spectrum internally calibrated using the matrix peaks. A more accurate mass of 1416.9 was obtained for the peptide in reflectron mode, a

TABLE 1. Mean levels of peptides measured with antisera F-4 and AS-10 in acetic acid extracts of G-E-P tissues in *M. nemestrina*

	ng equivalents S-28/mg protein					
RIA	Pancreas	Stomach	Duodenum	Jejunum	Ileum	Colon
F-4	7.7 ± 4[a]	16.2 ± 3[a]	48.8 ± 17	86.4 ± 10	83.6 ± 8	20.5 ± 3[a]
AS-10	28.4 ± 3	31.7 ± 9	33.3 ± 10	39.2 ± 6	45 ± 3	7.7 ± 3[a]
F-4/AS-10	0.3[a]	0.5[a]	1.5	2.2	1.9	2.7

Values represent mean ± SEM in tissues from four macaques.
[a] *Versus* mean values for jejunum; $P < 0.001$.

mass error of only 0.03%. To confirm the identity of the peptide species present in both reactive fractions as S-28$_{(1–13)}$, the masses of 1419.5 Da observed in the linear MALDI-TOF spectra were subjected to fragmentation by PSD. The PSD spectra obtained were compared with the PSD spectra obtained for pure, synthetic S-28$_{(1–13)}$ in which Met^{8} was oxidized to Met sulfoxide with H_2O_2. Despite the very low signal in the PSD spectra of the reactive fractions attributable to the extremely small amount of available peptide, approximately 10 fragment peaks were above the noise and in common with the strong fragment peaks observed in the PSD spectrum of oxidized synthetic S-28$_{(1–13)}$. Especially prominent were both y- and b-ions showing a neutral loss of 64 Da. A facile neutral loss of 64 Da corresponds to the loss of $SOCH_4$ and is indicative of Met sulfoxide in the peptide. Oxidation of the single Met residue present in S-28$_{(1–13)}$ is not unexpected, because of the harsh acidic extraction conditions used in processing the monkey tissue. Because F-4 antiserum has a much higher affinity (circa 50–100 fold) for S-28$_{(1–13)}$ than S-28 (Fig. 2), using this RIA with S-28 as standard led to an overestimate of the amount of material submitted for sequence and MS analyses. A reestimate suggests that 300–600 fmol were used in the N-terminal sequence analysis and 12–16 fmol for mass spectrometry. Despite the low levels of peptide, all 3 physical analyses (N-terminal sequence analysis, MALDI-TOF mass spectrometry, and PSD fragmentation) are consistent with the identity of the F-4 immunoreactive species as S-28$_{(1–13)}$.

Localization of F-4-containing cells and neurons in monkey G-E-P tissues

G-E-P tissues from the monkey and rat were immunostained with F-4 to identify cells producing the peptides containing its epitope S-28 and S-28$_{(1–13)}$ (Table 2). Antiserum F-4 produced bright immunofluorescence of pancreatic islet D cells compatible with the presence of ProS, and possibly S-28, within these cells (Fig. 6A). F-4 also stained enterocytes, and neural cell bodies and fibers distributed in the mucosal, submucosal, and muscularis regions of the gut wall (Fig. 6, C, E, G, and I). Although the results were qualitatively similar in the different regions of the small intestine, the ileum contained many more F-4-positive enterocytes and, particularly, neuronal elements, than the duodenum; and the numbers of F-4 positive cells gradually increased from upper to lower small intestine. In the mucosa, numerous brightly fluorescent F-4 reactive fibers coursed through and ramified into the tips of the villi (Fig. 6, C and E). In the submucosa, F-4-positive axons were distributed within the loose connective tissue and along blood vessels (Fig. 6E). In the myenteric plexus, a constellation of brightly fluorescent punctate structures resembling beaded fibers and terminals surrounded the neuronal perikarya in the myenteric ganglia (Fig. 6, G and I). Some neuronal perikarya in the myenteric and mesenteric plexuses showed cytoplasmic staining as well (Fig. 6, G and I). In contrast to the staining with F-4, antiserum AS-10, directed to a more C-terminal epitope of ProS, labeled only islet D cells (Fig. 6B) and intestinal mucosal cells (Fig. 6D), with minimal staining of neural elements (Fig. 6, F, H, and J).

To explore further where F-4 immunoreactivity colocalized with S-14 in the monkey and rat, two other antisera either specific for S-14 (AS-77) or cross-reactive with both S-14 and S-28 (MS-12) were also used. As summarized in Table 2, there were remarkable differences in the staining, with the antisera recognizing epitopes in the sequence of S-14, compared with F-4. As expected, there was strong immunoreactivity to AS-10, MS-12, and AS-77 in the pancreatic islets of *M. nemestrina* consistent with the presence of ProS-derived peptides, especially S-14. Enterocytes distributed in monkey intestinal villi were also stained by AS-10 and MS-12, but not by AS-77, confirming our previous observations in rats, which are compatible with the presence of S-28 but not S-14 within these endocrine cells (22, 23). By contrast, AS-10, MS-12, and AS-77 did not immunostain any of the neuronal cells or fibers in the intestine that were so prominently delineated by F-4. These results, which were similar in both paraffin and cryostat sections and duplicated in rat pancreas and intestine, demonstrate the presence of F-4-reacting material in cells that are not immunoreactive for S-14. We infer from this that S-28$_{(1–13)}$ is produced in some intestinal cells independent of peptides containing the C terminus of ProS.

F-4 immunoreactivity in Smst knockout mice

To determine whether the synthesis of S-28$_{(1–13)}$ is independent of PreproS gene expression, we compared the immunostaining characteristics of G-E-P cells in *Smst* −/− mice with those of control mice, using antisera reacting with domains throughout ProS. Wild-type mice had immunoreactivity to ProS-derived peptides in the expected regions of their pancreatic islets and GI tract (Fig. 7, Table 3). AS-10

TABLE 2. Semiquantitative distribution of cells showing fluorescence immunoreactivity for somatostatin-like peptides in pancreatic islets and small intestine (jejunum and ileum) of *M. nemestrina*

Antibody	Islet D cells	Mucosa		Submucosa	Muscularis		
		Enterocytes in villi	Nerve fibers in villi	Nerve cell bodies	Nerve fibers	Nerve cell bodies	Nerve fibers
F4	+++[a]	+++[a]	+++[a]	+[b]	+++[a]	+[b]	+++[a]
AS-77	+++[a]	—[d]	—[d]	—[d]	—[d]	—[d]	—[d]
AS-10	+++[a]	++[c]	—[d]	—[d]	—[d]	—[d]	—[d]
MS-12	+++[a]	++[c]	—[d]	—[d]	—[d]	—[d]	—[d]

[a] Many brightly staining cells or nerve fibers visible with 10× objective.
[b] Very few cells and dim staining, requiring 40× objective to detect.
[c] Few bright staining cells, most cells and fibers with dim staining.
[d] No cells or fibers detected.

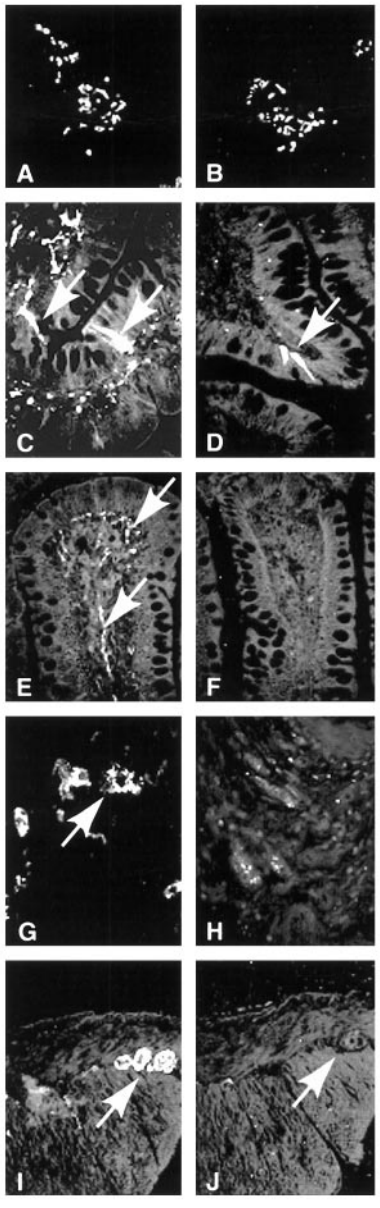

FIG. 6. Immunocytochemical localization of epitopes recognized by F-4 antiserum (A, C, E, G, and I) and AS-10 antiserum (B, D, F, H, and J) in pancreatic islets (A and B) and ileum (C–J) of *M. nemestrina*. Both antisera recognize epitopes in islet D cells (A and B) and in mucosal enterocytes (*small arrows* in C and D). F-4 recognizes nerve fibers in the mucosal villi (*large arrows* in C and *small arrows* in E), and neuronal cell bodies and fibers in the mesenteric (G) and myenteric (I) plexuses (examples of cell bodies indicated by *arrows*). However, AS-10 does not detect epitopes in any neural elements of the ileum (F, H, and J). Note that neuronal content of F-4 immunoreactivity in myenteric plexus neurons (I) (neurons indicated by *arrows*) is completely absent in an adjacent section immunostained with AS-10 (J). The same results were observed in jejunum and duodenum. The staining in H is nonspecific fluorescence. Controls showed no immunostaining in D cells, enterocytes, or neurons.

antiserum produced bright immunofluorescence of D cells in islets (Fig. 7A) and gastric mucosa (Fig. 7E) as well as of intestinal mucosal enterocytes and neuronal fibers of intestinal villi and submucosa (Fig. 7, I and M) but with minimal staining of cellular elements in the muscle wall of the gut (Fig. 7Q). The same results were obtained with CTP and Kiisha, more N-terminally reacting ProS antisera (data not shown). AS-77, which is specific for S-14, produced results similar to those of the other antisera, with the exception that it did not stain enterocytes, similar to the results presented above in monkey tissues (data not shown). In contrast to the control animals, the *Smst* knockout mice had no staining with S-14-specific antibodies [Fig. 7, B, F, J, N, and R; (21)].

In *Smst* +/+ mice, F-4 immunostained islet and gastric mucosal endocrine-like cells and enterocytes throughout the small intestine, in a pattern that was very similar to the one demonstrated in monkeys (Fig. 7, C, G, K, O, and S). In particular, F-4 immunostained neuronal fibers in mucosal villi and submucosa (Fig. 7, K and O), and unlike all the other ProS antisera, F-4-positive cell bodies (and to a lesser extent neuronal fibers) were observed in the myenteric plexus between the inner and outer smooth muscle layers of the intestinal wall (Fig. 7S). Remarkably, with the exception of islet D cells (Fig. 7D), all of the cell types that were identified by F-4 in the GI tissues of the *Smst* +/+ mice were also detected by F-4 in the *Smst* −/− mice (Fig. 7, H, L, P, and T; Table 3), indicating that an epitope recognized by F-4 was present despite the absence of other sequences of ProS. These results were consistent among all four wild-type and KO mice that were examined. Furthermore, the patterns of immunostaining were similar for tissues prepared by cryostat and paraffin processing and also by immunoperoxidase and immunofluorescent methods. The controls showed absence of immunostaining of all the above structures when primary antisera were omitted or replaced with normal serum. Nonspecific fluorescence or autofluorescence of these tissues was not present.

Molecular characterization of F-4 immunoreactivity from Smst +/+ and Smst −/− mice

Extracts of GI tissues from *Smst* −/− and *Smst* +/+ mice were fractionated by HPLC using a gradient that provided clear separation of S-28$_{(1–13)}$ and S-28 (Fig. 8). Extracts of stomach and upper and lower small intestine from the *Smst* −/− mice had peaks of F4-IR immunoreactivity that corresponded precisely to the elution position of synthetic S-28$_{(1–13)}$, whereas there was no F4 immunoreactivity at the later elution position of S-28. Intestinal extracts from the *Smst* +/+ mice also had an immunoreactive peak eluting at the position of the S-28$_{(1–13)}$ standard (data not shown). Samples of 0.1% TFA without added peptides, run after synthetic standard and tissue extracts, had no F4 immunoreactive peaks.

Discussion

In this paper, we describe the isolation of a peptide, from mammalian intestine, with a composition similar to the first 13 residues of S-28. However, despite its identity with the proximal sequence of S-28, our findings that it is dissociated from S-14 in neurons in the distal gut where it is in highest concentration, combined with evidence for its persistence in both endocrine and neuronal cells in the GI tract of mice in whom the PreproS gene has been eliminated, point to its derivation from a heretofore unrecognized gene. Although

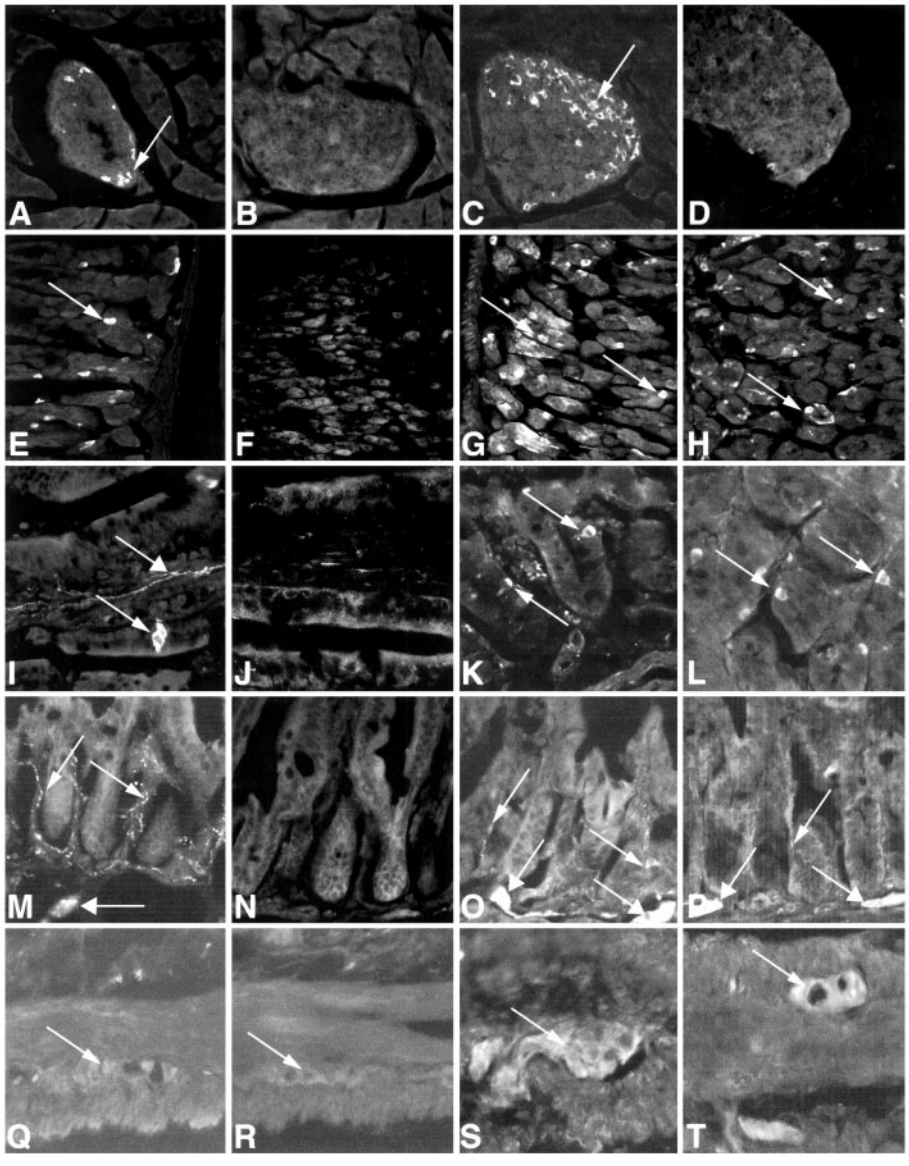

FIG. 7. Fluorescence immunocytochemical localization of cells recognized by AS-10 and F-4 antibodies in pancreatic islets (A–D), stomach (E–H), and small intestine (I–T) of *Smst* +/+ (wild-type) and *Smst* −/− (knockout) mice. Both AS-10 and F-4 stain islet D cells (some indicated by *arrows*) of *Smst* +/+ mice (A and C) but not *Smst* −/− mice (B and D). In stomach, AS-10 and F-4 stain mucosal D cells (some indicated by *arrows*) of *Smst* +/+ mice (E and G). These cells are not stained by AS-10 in *Smst* −/− animals (F) but are stained by F-4 (H). Similarly, mucosal enterocytes throughout the small intestine are recognized by AS-10 in *Smst* +/+ (I), but not in *Smst* −/−, mice (J), whereas F-4 stains mucosal enterocytes in both *Smst* +/+ (K) and *Smst* −/− (L) mice (enterocytes are indicated by *small arrows*; *large arrows* point to stained nerve fibers). Nerve fibers and cell bodies in villi and submucosa stain positively with AS-10 in *Smst* +/+ mice (M) but not in *Smst* −/− mice (N), whereas submucosal neurons are stained by F-4 in both *Smst* +/+ (O) and *Smst* −/− (P) rodents (*large arrows* indicate stained nerve fibers; enterocytes are indicted by *small arrows*). Neurons in the myenteric plexus of the muscularis layer (some *small arrows*) do not stain with AS-10 in either *Smst* +/+ (Q) or *Smst* −/− (R) mice, whereas F-4 stains myenteric plexus in both *Smst* +/+ (S) and *Smst* −/− (T) mice.

TABLE 3. Distribution of ProS-related immunostaining in G-E-P tissues of $Smst^{+}/Smst^{+}$ (+/+) wild type and $Smst^{-}/Smst^{-}$ (−/−) knockout mice

Phenotype	AS-10		AS-77		F-4		CTP		KIISHA	
	+/+	−/−	+/+	−/−	+/+	−/−	+/+	−/−	+/+	−/−
Pancreas										
Islet D cells	+	−	+	−	+	−	+	−	+	−
Stomach										
Gastric D cells	+	−	+	−	+	+	+	−	+	−
Small intestine										
Enterocytes	+	−	−	−	+	+	+	−	+	−
Mucosal neurons	+	−	+	−	+	+	+	−	+	−
Submucosal neurons	+	−	+	−	+	+	+	−	+	−
Myenteric neurons	−	−	−	−	+	+	−	−	−	−

we have purified this peptide from the intestine of macaques, the concordant findings of F-4 immunoreactivity in intestinal tissues of rats and mice suggest that it is also expressed in rodents. Because the gene has not been identified, nor has a function of the peptide been established, we have tentatively designated it as thrittene, based on the number of its residues and to distinguish it from peptides derived from the PreproS gene.

We initiated these studies to explain disparities between F-4 immunoreactivity and concentrations of S-28 determined

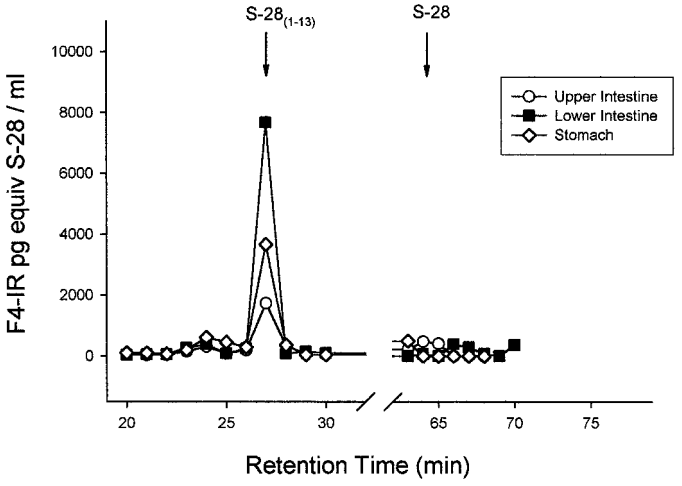

FIG. 8. HPLC profile of F-4 immunoreactive peptides (F-4 IR) from acetic acid extracts of the stomach and upper and lower small intestine of *Smst* −/− mice. Aliquots containing 150 μg protein were applied to a C-18 rp column with a variable gradient of CH_3CN in 0.1% TFA. Fractions were collected at 1-min intervals and analyzed in the F4 RIA. Synthetic S-$28_{(1–13)}$ eluted as a peak (detected either by absorbance of UV light or by F4 RIA) at 27 min, and S-28 at 65 min.

by a two-step immunoassay in plasma and tissue. In pursuing this observation, we identified an F-4 immunoreactive moiety with characteristic and reproducible chromatographic properties, whether obtained from plasma or intestinal extracts. Based on gel exclusion chromatography, this substance appeared to be larger than S-28; but, in fact, subsequent analyses showed that the F-4 immunoreactive peak immediately preceding S-28 eluted at the position identical to synthetic S-$28_{(1–13)}$. We were able to confirm the implications of the first chromatographic studies by HPLC, peptide sequencing, and mass spectrometry. The partial sequence of the 13-residue peptide that was obtained from material purified from monkey intestine is consistent with 8 of the 13 interspersed residues in correct sequence with that of S-$28_{(1–13)}$ and contains the epitope that we had previously shown to be required for interaction with F-4 (17). The C-terminal amino acid was not determined; thus, we cannot be absolutely certain that it is Arg. However, the mass of 1416.9 Da for the isolated peptide obtained by MALDI-TOF MS analysis and the behavior of the isolate after PSD fragmentation are precisely those predicted, and proven, for authentic S-$28_{(1–13)}$ with an oxidized methionine residue. Thus, we are confident that the sequence we have assigned this peptide is correct.

Based on the inverse molar ratio of F-4 and AS-10 immunoreactivity in extracts along the GI tract, thrittene is present in highest concentrations in the distal segments of the gut, in contrast to S-14 and S-28, which we and others have shown to be most prevalent in the stomach and upper small intestine (22, 24–27). Because all peptides containing the C terminus of ProS are recognized by AS-10, the relative increase in F-4 immunoreactivity cannot be explained by a preponderance of S-28 over S-14 in this region. Our immunocytochemical results amplify this point by locating F-4 reacting cells in a neuronal network in the mucosa and submucosa of the jejunum and ileum that do not stain with AS-10 and MS-12 or an antiserum highly specific for S-14 (AS-77). Though we cannot exclude the possibility that ProS and thrittene are coexpressed in some tissues, these data indicate that both endocrine and neuronal cells in the GI tract also produce thrittene independent of ProS-derived peptides. This finding is consistent with derivation of thrittene from a gene other than PreproS.

Though the nucleic acid sequence corresponding to thrittene is not known, the data presented herein support a novel gene precursor. First, we have been unable to identify a DNA sequence, other than ProS, that corresponds with the sequence of S-$28_{(1–13)}$ using computer driven searches of current data banks. Second, the comparative F-4 RIA measurements in tissue extracts, coupled with the results of immunocytochemistry, suggest that thrittene is synthesized independent of the ProS-derived peptides. Third, the persistent F-4 immunoreactivity, demonstrated both by immunostaining and after extraction of peptides, in the GI endocrine and neuronal cells of mice homozygous for the *Smst* null allele indicates that thrittene is produced in the absence of ProS. The *Smst* −/− animals have a deletion of promoter sequences and the first exon of the PreproS gene that includes the transcriptional start site and encodes a major portion of the N terminus of ProS (21). Though exon 2 encoding the C terminus of ProS is present in the mice, the absence of detectable ProS mRNA, assessed either by RT-PCR or *in situ* hybridization, and the complete lack of ProS derived peptides, assessed either by immunocytochemistry or by RIA of tissue extracts, indicates the fidelity of the knockout of the PreproS gene in these animals (21). The distribution of F-4 immunoreactivity in GI cells in the knockout mice, similar to those that were stained in monkeys and rats and wild-type mice, indicates that thrittene synthesis is shared by both endocrine cells in stomach and gut and neurons predominating in the myenteric plexus.

The somatostatin-related peptides are ubiquitous among animals, and there is evidence that at least 1 duplication of PreproS persists in the mammalian genome (1). Anglerfish, from which ProS was first cloned, and frogs have 2 somatostatin genes (1, 28), as do several other species. Cortistatin, a recently discovered peptide that shares 11 of 14 residues with S-14, is the product of a separate gene (3, 4). Prepro-cortistatin has only limited homology with ProS beyond the C terminus, but these genes are considered to be related; and so, they may derive from a common ancestor. Given the significant concordance between thrittene and the proximal region of S-28, it is possible that the gene encoding thrittene is also related to PreproS. Clearly, the placement of thrittene among known families of regulatory peptides awaits the ascertainment of its DNA sequence.

To our knowledge, this paper contains the first description of thrittene as a distinct entity; nonetheless, it is possible that previous investigators of ProS and its processing may have unwittingly come upon this peptide. Two groups have described antisera that they believed to be specific for the epitopes containing the C-terminal Glu residue shared by S-$28_{(1–12)}$ and $ProS_{(1–76)}$ (14, 20). These antisera, designated S-320 by Benoit *et al.* (20) and R-109 by Patel *et al.* (14), were tested for cross-reactivity with several congeners of S-28. However, S-$28_{(1–13)}$ was not included among the published

reports; therefore, we infer that it was not evaluated. In our hands, S-28$_{(1–13)}$ and S-28$_{(1–12)}$ interacted equally with S-320 (data not shown). Furthermore, because the peptides differ by only one residue, they could easily be mistaken for one another unless special attention was given to methods for their separation. Thus, it is plausible that thrittene may have been included in the measurements attributed to S-28$_{(1–12)}$ when antiserum S-320 was used for RIA of extracts from brain and G-E-P tissues (14, 20). This may also explain the discrepancy noted when Morrison and colleagues immunostained mammalian neocortical cells with S-320 and other immune sera interacting specifically with S-14 and S-28 (29). In these studies that were replicated by Lewis *et al.* (30), staining with S-320 was widespread in neuronal processes, terminals, and dendrites, whereas S-28 was localized to some cell bodies, but virtually no S-14 was observed. Although an explanation for these findings was never published, it is possible that some of the neocortical neurons that were stained with S-320 contained thrittene exclusively, analogous to our findings with F-4 in intestinal neurons. Though we have not yet examined brain tissue for immunocytochemical evidence of thrittene, it is reasonable to postulate that thrittene is also present in the CNS, because it is common for peptides expressed in the GI tract to be found also in the brain.

Based on the immunostaining of gastric and enteric endocrine-like cells in the *Smst* −/− mice, the major source of thrittene in human (and nonhuman primate) plasma is presumed to be endocrine cells in the stomach and distal small intestine. We have found that plasma concentrations of thrittene increased 2- to 3-fold in humans after ingestion of a mixed meal (Ensinck, J. W., unpublished observation). Because fat and, to a lesser extent, carbohydrate evoked this release, secretion of thrittene is likely to be regulated by specific nutrients similar to other GI peptides. Traditionally, peptides that are secreted from cells within GI tissues in response to food intake originate in cells of epithelial origin and act as hormones on distant targets (31). Thus, it is reasonable to deduce that the presence of thrittene in plasma reflects its secretion from GI endocrine cells. As yet, we have no clear-cut evidence for a biologic effect of this putative hormone/neurotransmitter on G-E-P functions; however, we have observed that, when instilled into the cerebral ventricles of rats, thrittene decreases food intake in a dose-dependent manner without evoking an aversive response (32).

In summary, we have immunological and physical evidence of the existence of a peptide with mass of 1416.9 Da and a partial sequence compatible with the assignment of a structure of S-28$_{(1–13)}$. We isolated this peptide from the distal intestine of nonhuman primates and demonstrated, by RIA of tissue extracts and immunocytochemistry, that it is located in endocrine cells in stomach and intestine and in myenteric neurons that do not contain ProS. On the basis of persistence of immunoreactivity in GI cells of *Smst* −/− mice and the lack of a corresponding DNA sequence in previously reported genes, we deduce that thrittene is derived from a hitherto-unrecognized gene.

Acknowledgments

We appreciate the excellent technical assistance of Joyce Murphy and Chare Vathanaprida for tissue fixation and immunostaining.

Received July 10, 2001. Accepted March 21, 2002.

Address all correspondence and requests for reprints to: David D'Alessio, M.D., University of Cincinnati, Division of Endocrinology, ML 0547, Cincinnati, Ohio 45267-0547. E-mail: david.d'alessio@uc.edu.

This work was supported by NIH Grants DK-34397 (to J.W.E.), DK-02305 (to D.D.), RR00037 (University of Washington General Clinical Research Center), RR-00166 (University of Washington Regional Primate Research Center), and DK-34397 (University of Washington Diabetes and Endocrine Research Center). Additional support was provided by grants from the American Diabetes Association (to D.D.), the Juvenile Diabetes Foundation (to J.W.E.), Merit Review and Career Scientist awards from the Department of Veterans Affairs (to D.G.B.), and a grant from the Medical Research Foundation of Oregon (to M.J.L.).

* Present address: R. W. Johnson Pharmaceutical Research Institute, Route 202, P.O. Box 300, Raritan, New Jersey 08869-0602.

† Present address: Howard Hughes Medical Institute, University of California at San Diego, Mailstop 0314, 9500 Gilman Drive, La Jolla, California 92103-0314.

‡ Present address: Argonex, Inc., 706 Forest Street, Suite 1, Charlottesville, Virginia.

§ Present address: Instituto de Investigaciones en Ingeneria Genetica y Biologia Molecular, Consejo Nacional de Investigaciones Científicas y Técnicas de Argentina, and Departamento de Ciencias Biológicas, Facultad de Ciencias Exactas y Naturales, University of Buenos Aires, 1428 Buenos Aires, Argentina.

References

1. **Conlon JM, Tostivint H, Vaudry H** 1997 Somatostatin- and urotensin II-related peptides: molecular diversity and evolutionary perspectives. Regul Pept 69:95–103
2. **Argos P, Taylor WL, Minth CD, Dixon JE** 1983 Nucleotide and amino acid sequence comparisons of preprosomatostatins. J Biol Chem 258:8788–8793
3. **de Lecea L, Criado JR, Prospero-Garcia O, Gautvik KM, Schweitzer P, Danielson PE, Dunlop CL, Siggins GR, Henriksen SJ, Sutcliffe JG** 1996 A cortical neuropeptide with neuronal depressant and sleep-modulating properties. Nature 381:242–245
4. **Spier AD, de Lecea L** 2000 Cortistatin: a member of the somatostatin neuropeptide family with distinct physiological functions. Brain Res Brain Res Rev 33:228–241
5. **Patel YC** 1992 General aspects of the biology and function of somatostatin. In: Thorner MO, Muller EE, eds. Basic and clinical aspects of neuroscience. Berlin: Springer-Verlag; vol 4:1–16
6. **Patel YC** 1999 Somatostatin and its receptor family. Front Neuroendocrinol 20:157–198
7. **Patel YC, Galanopoulou A** 1995 Processing and intracellular targeting of prosomatostatin-derived peptides: the role of mammalian endoproteases. Ciba Found Symp 190:26–50
8. **Beinfeld MC, Bourdais J, Kuks P, Morel A, Cohen P** 1989 Characterization of an endoprotease from rat small intestinal mucosal secretory granules which generates somatostatin-28 from prosomatostatin by cleavage after a single arginine residue. J Biol Chem 264:4460–4465
9. **Gluschankof P, Gomez S, Morel A, Cohen P** 1987 Enzymes that process somatostatin precursors. A novel endoprotease that cleaves before the arginine-lysine doublet is involved in somatostatin-28 convertase activity of rat brain cortex. J Biol Chem 262:9615–9620
10. **Gomez S, Gluschankof P, Lepage A, Cohen P** 1988 Relationship between endo- and exopeptidases in a processing enzyme system: activation of an endoprotease by the aminopeptidase B-like activity in somatostatin-28 convertase. Proc Natl Acad Sci USA 85:5468–5472
11. **Galanopoulou AS, Seidah NG, Patel YC** 1995 Direct role of furin in mammalian prosomatostatin processing. Biochem J 309:33–40
12. **Galanopoulou AS, Kent G, Rabbani SN, Seidah NG, Patel YC** 1993 Heterologous processing of prosomatostatin in constitutive and regulated secretory pathways. Putative role of the endoproteases furin, PC1, and PC2. J Biol Chem 268:6041–6049
13. **Patel YC** 1983 A high molecular weight form of somatostatin-28 (1–12)-like immunoreactive substance without somatostatin-14 immunoreactivity in the rat pancreas. Evidence that somatostatin-14 synthesis can occur independently of somatostatin-28. J Clin Invest 72:2137–2143
14. **Patel YC, O'Neil W** 1988 Peptides derived from cleavage of prosomatostatin at carboxyl- and amino-terminal segments. Characterization of tissue and secreted forms in the rat. J Biol Chem 263:745–751

15. **Brakch N, Rholam M, Nault C, Boileau G, Cohen P** 1991 Differential processing of hormone precursor. Independent production of somatostatins 14 and 28 in transfected neuroblastoma 2A cells. FEBS Lett 282:363–367
16. **Holst JJ, Baldissera FG, Bersani M, Skak-Nielsen T, Seier-Poulsen S, Nielsen OV** 1988 Processing and secretion of prosomatostatin by the pig pancreas. Pancreas 3:653–661
17. **Ensinck J, Laschansky E, Vogel R, Siminowitz D, Roos B, Francis B** 1989 Circulating prosomatostatin-derived peptides: differential responses to food ingestion. J Clin Invest 83:1580–1589
18. **Ensinck JW, Vogel RE, Laschansky EC, Koerker DJ, Prigeon RL, Kahn SE, D'Alessio DA** 1997 Endogenous somatostatin-28 modulates postprandial insulin secretion. Immunoneutralization studies in baboons. J Clin Invest 100: 2295–2302
19. **Aron DC, Andrews PC, Dixon JE, Roos BA** 1984 Identification of cellular prosomatostatin and nonsomatostatin peptides derived from its amino terminus. Biochem Biophys Res Commun 124:450–456
20. **Benoit R, Ling N, Alford B, Guillemin R** 1982 Seven peptides derived from pro-somatostatin in rat brain. Biochem Biophys Res Commun 107:944–950
21. **Low MJ, Otero-Corchon V, Parlow AF, Ramirez JL, Kumar U, Patel YC, Rubinstein M** 2001 Somatostatin is required for masculinization of growth hormone-regulated hepatic gene expression but not of somatic growth. J Clin Invest 107:1571–1580
22. **Francis BH, Baskin DG, Saunders SR, Ensinck JW** 1990 Distribution of somatostatin-14 and somatostatin-28 gastrointestinal-pancreatic cells of rats and humans. Gastroenterology 99:1283–1291
23. **Baskin DG, Ensinck JW** 1984 Somatostatin in epithelial cells of intestinal mucosa is present primarily as somatostatin 28. Peptides 5:615–621
24. **Vinik AI, Gaginella TS, O'Dorisio TM, Shapiro B, Wagner L** 1981 The distribution and characterization of somatostatin-like immunoreactivity in epithelial cells, submucosa, and muscle of the rat stomach and intestine. Endocrinology 109:1921–1926
25. **Patel YC, Wheatley T, Ning C** 1981 Multiple forms of immunoreactive somatostatin: comparison of distribution in neural and nonneural tissues and portal plasma of the rat. Endocrinology 109:1943–1949
26. **Penman E, Wass JA, Butler MG, Penny ES, Price J, Wu P, Rees LH** 1983 Distribution and characterisation of immunoreactive somatostatin in human gastrointestinal tract. Regul Pept 7:53–65
27. **Baldissera FG, Holst JJ, Jensen SL, Krarup T** 1985 Distribution and molecular forms of peptides containing somatostatin immunodeterminants in extracts from the entire gastrointestinal tract of man and pig. Biochim Biophys Acta 838:132–143
28. **Noe BD, Spiess J** 1983 Evidence for biosynthesis and differential post-translational proteolytic processing of different (pre)prosomatostatins in pancreatic islets. J Biol Chem 258:1121–1128
29. **Morrison JH, Benoit R, Magistretti PJ, Bloom FE** 1983 Immunohistochemical distribution of pro-somatostatin-related peptides in cerebral cortex. Brain Res 262:344–351
30. **Lewis DA, Campbell MJ, Morrison JH** 1986 An immunohistochemical characterization of somatostatin-28 and somatostatin-281–12 in monkey prefrontal cortex. J Comp Neurol 248:1–18
31. **Rehfeld JF** 1998 The new biology of gastrointestinal hormones. Physiol Rev 78:1087–1108
32. **D'Alessio DA, Rushing PA, Blake K, Ensinck JW, Seeley RA** 2000 Suppression of food intake by Somatostatin-28(1–13) a novel gut peptide. Diabetes 49:A260